RAPID PUBLICATION

Electrical Coupling: Novel Mechanism for Sleep-Wake Control

Edgar Garcia-Rill, PhD; David S. Heister, BS; Meijun Ye, BMed; Amanda Charlesworth, PhD; Abdallah Hayar, PhD

Center for Translational Neuroscience, Department of Neurobiology & Dev. Sci., University of Arkansas for Medical Sciences, Little Rock, AR

Study Objectives: Recent evidence suggests that certain anesthetic agents decrease electrical coupling, whereas the stimulant modafinil appears to increase electrical coupling. We investigated the potential role of electrical coupling in 2 reticular activating system sites, the subcoeruleus nucleus and in the pedunculopontine nucleus, which has been implicated in the modulation of arousal via ascending cholinergic activation of intralaminar thalamus and descending activation of the subcoeruleus nucleus to generate some of the signs of rapid eye movement sleep.

Design: We used 6- to 30-day-old rat pups to obtain brainstem slices to perform whole-cell patch-clamp recordings.

Measurements and Results: Recordings from single cells revealed the presence of spikelets, manifestations of action potentials in coupled cells, and of dye coupling of neurons in the pedunculopontine nucleus. Recordings in pairs of pedunculopontine nucleus and subcoeruleus nucleus neurons revealed that some of these were electrically coupled with coupling coefficients of approximately 2%. After blockade of fast synaptic transmission, the cholinergic agonist carbachol was found to induce rhythmic activity in pedunculopontine nucleus and subcoeruleus nucleus neurons, an effect eliminated by the gap junction blockers carbenoxolone or mefloquine. The stimulant modafinil was found to decrease resistance in neurons in the pedunculopontine nucleus and subcoeruleus nucleus after fast synaptic blockade, indicating that the effect may be due to increased coupling.

Conclusions: The finding of electrical coupling in specific reticular activating system cell groups supports the concept that this underlying process behind specific neurotransmitter interactions modulates ensemble activity across cell populations to promote changes in sleep-wake state.

Keywords: Arousal, carbachol, connexin 36, gap junctions, modafinil, pedunculopontine, subcoeruleus.

Citation: Garcia-Rill E; Heister DS; Ye M; Charlesworth A; Hayar A. Electrical coupling: novel mechanism for sleep-wake control. *SLEEP* 2007;30(11):1405-1414.

THE PEDUNCULOPONTINE NUCLEUS (PPN), THE CHOLINERGIC ARM OF THE RETICULAR ACTIVATING SYSTEM (RAS), CONTAINS MEDIUM AND LARGE CHOLINERGIC neurons as well as small noncholinergic cells[1] and has both ascending and descending projections. Early work established that electrical stimulation of the region of the PPN induced desynchronization of the electroencephalogram, similar to that seen during waking and rapid eye movement (REM) sleep.[2] PPN neurons show increased rates of firing during waking and REM sleep, but fire less during slow wave sleep.[3] Lesions of the PPN[4,5] or pharmacologic blockade of PPN efferents[6] decrease or eliminate REM sleep and diminish waking. Fast cortical oscillations in waking and REM sleep are triggered by PPN depolarization (push) of thalamocortical relay neurons via muscarinic inhibition of a K^+ conductance, whereas PPN hyperpolarization (pull) of reticular thalamic neurons blocks spindles.[7] In addition, the majority of PPN neurons project to the "nonspecific" intralaminar thalamus,[8] especially the parafascicular nucleus in primates.[9] The "nonspecific" thalamic system, including the parafascicular nucleus, is thought to allow sensory input to access the machinery that presumably generates conscious experience, the thalamocortical 40-Hz rhythm.[10]

The PPN also sends descending projections throughout the pontomedullary reticular formation, including the anterior pontine region.[11,12] Injections of cholinergic agonists into a region called the pontine inhibitory area induce signs of a REM sleep-like state (atonia and pontogeniculooccipital waves, depending on species and preparation).[13,14] Lesioning of this pontine region, termed the subcoeruleus, can produce REM sleep without atonia or decreases in REM sleep signs.[15-17] Recent studies on subcoeruleus cells reported neurons excited by the cholinergic agonist carbachol (presumed to be REM-on cells) with low threshold spikes (LTS) and cells inhibited by carbachol, some with LTS, some with Ia current.[18]

We observed the presence of spikelets and dye coupling in neurons in the PPN and subcoeruleus and recently published indirect evidence for electrical coupling in the subcoeruleus.[19] The present study was conducted to provide direct evidence of electrical coupling in the PPN and subcoeruleus by recording from pairs of coupled neurons and to study correlated activity between these cells, especially that induced by carbachol.

Electrical coupling in the mammalian brain was first described in the 1970s, with connexin 36 (Cx36) being the only gap junction protein between neurons.[20] Spikelets are stereotypical, usually rhythmic, subthreshold depolarizing potentials thought to reflect synchronous firing in the coupled neurons, as opposed to noncoupled cells.[21] Electrical synapses appear mainly between GABAergic neurons in the thalamic reticular nucleus and in the cortex, where they may enhance the synchrony of gamma oscillations.[22,23] A recent report suggests that the stimulant modafinil acts by increasing electrical coupling in cortical, reticular thalamic, and inferior olive neurons.[24] Our results demonstrate the presence of coupled neurons in RAS neurons of the PPN and subcoeruleus, and their modulation by carbachol and modafinil to induce oscillations, emphasizing the role of electrical coupling as a novel mechanism for sleep-wake control. Preliminary findings have been reported in abstract form.[25]

Disclosure Statement

This is not an industry supported study. Dr. Garcia-Rill has received research support from Sepracor and has financial interests in BMI Inc. The other authors have reported no financial conflicts of interest.

Submitted for publication July, 2007
Accepted for publication August, 2007

Address correspondence to: E. Garcia-Rill, PhD, Professor and Director, Center for Translational Neuroscience, Department of Neurobiology & Dev. Sci., University of Arkansas for Medical Sciences, 4301 West Markham St., Slot 847, Little Rock, AR 72205; Tel: (501) 686-5167; Fax: (501) 526-7928; E-mail: GarciaRillEdgar@uams.edu

METHODS

All of the methods used were the same as those previously published in a limited study of the subcoeruleus.[19] Pups aged 7 to 20 days from adult timed-pregnant Sprague-Dawley rats (280-350 g) were anesthetized with ketamine (70 mg/kg, intramuscularly) until the tail-pinch reflex was absent. They were decapitated, and the brain rapidly removed and cooled in oxygenated sucrose-artificial cerebrospinal fluid (sucrose-aCSF). The sucrose-aCSF consisted of (in mM): 233.7 sucrose, 26 $NaHCO_3$, 8 $MgCl_2$, 0.5 $CaCl_2$, 20 glucose, 0.4 ascorbic acid, and 2 sodium pyruvate. Coronal and parasagittal sections (400 μm) containing the subcoeruleus and the pedunculopontine nucleus were cut and initially placed in 30°C aCSF before they were allowed to equilibrate to room temperature for 1 hour. The aCSF was composed of (in mM) NaCl 117, KCl 4.7, $MgSO_4$ 1.2, $CaCl_2$ 2.5, NaH_2PO_4 2.8, $NaHCO_3$ 24.9, and glucose 11.5. Slices were recorded at 30°C while superfused (1.5 mL/min) with oxygenated (95% O_2- 5% CO_2) normal aCSF. Differential interference contrast optics was used to visualize neurons using an upright microscope (Nikon Eclipse FN-1, Nikon, Melville, NY).

Whole-cell recordings were acquired using borosilicate glass capillaries pulled on a P-97 puller (Sutter Instrument Company, Novato, CA) and filled with a solution of (in mM) 124 K-gluconate, 10 HEPES, 10 phosphocreatine di tris, 0.2 EGTA, 4 Mg_2ATP, 0.3 Na_2GTP, and 0.02% Lucifer yellow or 0.3% Neurobiotin (Vector Laboratories). Osmolarity was adjusted to approximately 270 to 290 mOsm and pH to 7.4. The pipette resistance was 5 to 8 MΩ. All recordings were made using a Multiclamp 700B amplifier (Axon Instruments, Foster City, CA). Analog signals were low-pass filtered at 2 kHz (Multiclamp 700B) and digitized at 5kHz using a Digidata-1322A and pClamp9 software (Axon instruments, Foster City, CA). Off-line analyses were performed using Clampfit software (Axon Instruments). Drugs were applied to the slice via a peristaltic pump (Cole-Parmer, Vernon Hills, IL) and a 3-way valve system. Carbachol (20-50 μM), carbenoxolone (300 μM), mefloquine (mefloquine, 20 μM), modafinil (modafinil, 100-200 μM), 6-cyano-7-nitroquinoxaline-2, 3-dione (CNQX, 10 μM), gabazine (10 μM), strychnine (10 μM), and (±)-2-amino-5-phosphopentanoic acid (APV, 10μM) and tetrodotoxin (TTX, 1 μM), were all purchased from Sigma (St. Louis, MO), except for mefloquine, which was obtained from the National Institutes of Health. CNQX, APV, strychnine and gabazine are termed herein as fast synaptic blockers.

The locations of recorded cells were determined using histologic verification of neurobiotin or Lucifer yellow injected cells. All PPN neurons were located in the region of NADPH diaphorase-positive cells (determined using standard histochemical labeling), and most subcoeruleus neurons were located anterior to the seventh nerve in the region of the rat brainstem termed dorsal subcoeruleus. Although tyrosine hydroxylase immunocytochemistry was not performed, most recordings were well ventral to the locus coeruleus where only scattered tyrosine hydroxylase-positive neurons are found, and the subcoeruleus neurons studied did not show typical catecholaminergic action potential shape and firing properties.

To determine the levels of Cx36 protein in the PPN and subcoeruleus, we cut 400-μm sagittal sections, such as those used for recordings, and punched (1 mm) the PPN and subcoeruleus in 10-day and 30+day animals from each of 4 additional litters. For Cx36 protein analysis, tissue was homogenized in RIPA buffer (50 mM Tris-Cl, pH 7.5, 150 mM NaCl 1% NP-40, 0.5%, Na-deoxycholate, 0.1% SDS) with HALT protease inhibitor cocktail (Pierce), and cell debris was removed by centrifugation. Fifteen micrograms per lane of protein was separated by SDS-PAGE and transferred onto nitrocellulose. Blots were blocked in 5% nonfat milk in TBS (Tris-buffered saline: 20 mM Tris-Cl, pH 7.5, 150 M NaCl) overnight at 4°C. Anti-Cx36 antibodies (#51-6300, Invitrogen) were used at 1:250 in TBST (TBS with 0.05% Tween-20) with 1% milk for 4 hours, at 25°C. Anti-rabbit IgG-HRP (Promega) was used at 1:2,500 in TBST for 1 hour at 25°C. Proteins were visualized using Chemiglow West (Alpha Innotech) and light emission captured by a Fluorchem SP (Alpha Innotech). Blots were stripped with Restore™ (Pierce) and reprobed with antibodies against ß-tubulin (Sigma) to verify equal protein loading. AlphaEase software was used to quantify the amount of Cx36 and tubulin protein in the PPN and subcoeruleus.

For comparison of data between the different groups in each experiment, measures were tested using one factor analysis of variance to conclude whether any of the factors has a significant effect on the magnitude of the variable and also whether the interaction of the factors significantly affects the variable. Differences were considered significant at values of $P \leq 0.05$. If statistical significance was present, the Scheffe posthoc test was used to compare between groups.

RESULTS

PPN Recordings

Previous intracellular recordings had revealed the presence of spontaneous spikelets in PPN neurons.[25] In the present study, we observed that 19% of patch-clamped PPN neurons showed spontaneous spikelets and an additional 8% showed spikelets in the presence of carbachol (50 μM). We recorded from a total of 53 PPN neurons for this study, including 3 pairs of electrically coupled cells. Figure 1A is an example of paired recordings from 2 PPN neurons. In the presence of TTX (1 μM) to block synaptic transmission, hyperpolarizing pulses delivered to 1 cell induced a current in the other cell, and vice versa. The coupling ratio in the paired recordings was calculated as the amplitude of the current generated in the coupled cell divided by the amplitude of the current induced in the injected cell during application of a -50-mV voltage step. The mean ± SEM of the coupling ratio of PPN cells was 1.4% ± 0.5%. In addition, we recorded 39 individual PPNcells after superfusion with fast synaptic blockers (CNQX 10 μM, APV 50 μM, gabazine 10 μM) and found that 4 of 39 showed rhythmic oscillations in the presence of carbachol (50 μM). An example of the carbachol-induced oscillation in the presence of fast synaptic blockers (+ the nicotinic receptor blocker MEC 10 μM) is shown in Figure 1B and C. The oscillations induced by carbachol in the PPN were in the 4- to 8+Hz frequency range. In some PPN cells, the effects of gap junction modulators were tested. Figure 1B and C shows that the gap junction blocker carbenoxolone (300 μM) eliminated the carbachol-induced oscillations in a PPN neuron. We also tested the effects of the stimulant modafinil on the input resistance in 25 PPN cells. Figure 1D shows the decrease in input resistance induced by modafinil in a PPN cell, an effect partially reversed by the putative gap junction blocker mefloquine (25 μM).

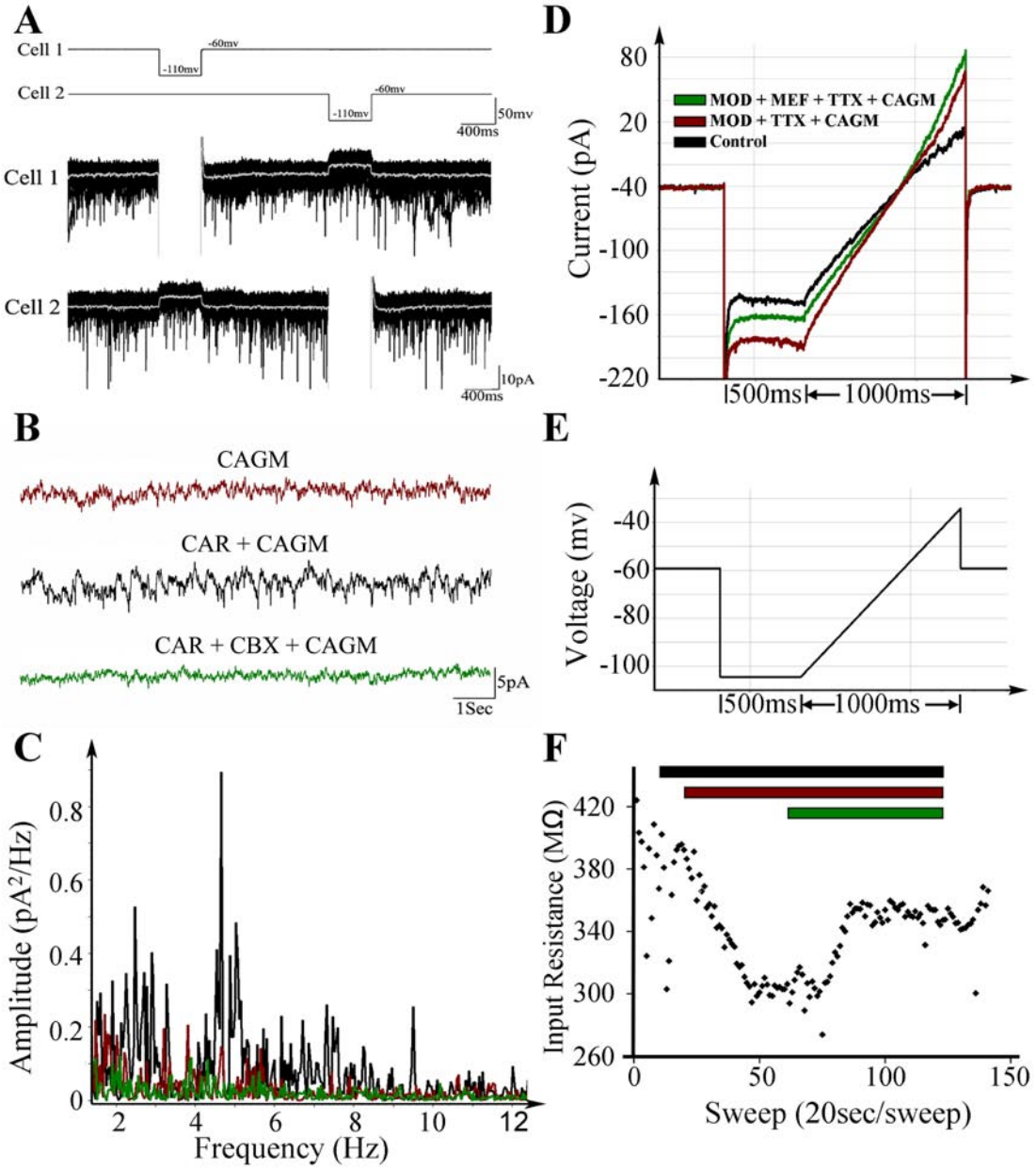

Figure 1—Modulation of electrical couplings in the pedunculopontine nucleus (PPN). **A**. Whole-cell patch-clamp recordings from a pair of electrical coupled PPN neurons under voltage clamp. Hyperpolarizing pulses (top 2 records show current pulses) injected to 1 cell induced a current in the other cell in the presence of 1 μM tetrodrotoxin (TTX) to block sodium channels and thus action potential generation. The coupling ratio was calculated using the current amplitude in the injected cell divided by the response current in the coupled cell. For this pair, the coupling ratio of cell 1 to cell 2 was 1.6%, and of cell 2 to cell 1 was 2%. The gray line represents the average of 20 sweeps after a 3-minute superfusion of TTX. **B**. No significant activity was present in this cell during superfusion of fast inhibitory and excitatory synaptic blockers (CAGM = 6-cyano-7-nitroquinoxaline-2, 3-dione [CNQX] 10 μM, (±)-2-amino-5-phosphopentanoic acid [APV] 10 μM, gabazine 10 μM, and mecamylamine 10 μM) (top record). Carbachol (CAR, 50 μM) induced oscillations in this PPN cell in the presence of fast inhibitory and excitatory synaptic blockers (CAGM) (second record), which was blocked by 300 μM carbenexolone (CBX), a putative gap junction blocker (bottom record). **C**. Power spectrum histogram of the oscillations induced by fast synaptic blockers (no discernible synchronization), CAR in the presence of fast synaptic blockers (theta frequency oscillations), and their blockade by CBX in the same cell shown in B. Each histogram was obtained from a 1-minute recording sample. **D**. An example of a PPN cell whose input resistance was decreased by fast synaptic blockers (CAGM), then decreased further by the superfusion of modafinil (MOD, 150 μM) in the presence of fast synaptic blockers (CAGM). The decrease in resistance was partially reversed by the putative gap junction blockers mefloquine (MEF, 25 μM). The cell was recorded under voltage-clamp mode. A ramp protocol was applied in order to test the change of membrane resistance, such that a higher current was required to compensate for the voltage change in the presence of modafinil, indicating a decrease in resistance. **E**. The ramp protocol used in the recording shown in D. The voltage was held at -60 mV during baseline and then was held at -105 mV for 500 milliseconds. to test the compensatory current. A 1000-millisecond ramp from -105 mV to -35 mV was then applied. **F**. The membrane resistance change during 50-minute recording from the same cell shown in D. The bars indicate the period when drugs were applied (black: 1 μM TTX + 10 μM CAGM; maroon: 150 μM MOD + TTX + CAGM; green: 25 μM MEF + TTX + CAGM). The resistance was calculated by dividing voltage change by the compensatory current.

Of the 39 PPN cells tested, 18 (50%) were depolarized by carbachol, 16 were hyperpolarized, and 5 were not affected. When PPN cells were divided according to cell type (type I: LTS current; type II: Ia current; type III: Ia+LTS currents), of the cells depolarized, 1 of 18 was type I, 13 of 18 were type II, and 4 of 18 were type III. Of the cells hyperpolarized, 3 of 16 were type I, 12 of 16 were type II, and 1 of 16 was type III. Of the cells not affected, 1 of 5 was type I, 3 of 5 were type II, and 1 of 5 was type III. Of the cells that were induced to oscillate by carbachol, 2 were type I, 2 were type II, and no type III cells oscillated.

Figure 2 shows the effects of carbachol, fast synaptic blockers, and gap junction blockers on synchronized activity in a pair of PPN neurons. In this case, loose patch extracellular recordings were made from a pair of PPN neurons that showed some correlated activity, suggesting that they were coupled. When carbachol was added, their activity increased or decreased, but the cross-correlation coefficient always increased. When carbachol was added in the presence of fast synaptic blockers (suggesting that correlated firing could be mediated only by gap junctions), the carbachol-induced cross-correlation increased dramatically, showing virtually coincident firing patterns. The cross-correlation was completely blocked by the addition of the gap junction blocker carbenoxolone.

Subcoeruleus Recordings

Figure 3A shows the occurrence of spikelets in a subcoeruleus neuron and their distinction from excitatory postsynaptic currents. We found that 6 subcoeruleus cells showed spontaneous spikelets and 10 exhibited spikelets in the presence of carbachol (50 μM). We recorded from a total of 178 subcoeruleus neurons for this study, including 3 pairs of electrically coupled cells. Figure 3B is an example of paired recordings from 2 subcoeruleus neurons. In the presence of TTX (1 μM) to block synaptic transmission, hyperpolarizing pulses delivered to 1 cell induced a current in the other cell, and vice versa. The mean ± SEM of the coupling ratio of subcoeruleus cells was 3.1% ± 0.8%. In addition, we recorded 34 individual subcoeruleus cells after superfusion with fast synaptic blockers (CNQX, APV, gabazine, 10 μM) and found that 8 of 34 showed rhythmic oscillations in the presence of carbachol (50 μM). An example of the carbachol-induced oscillation is shown in Figure 3C. The oscillations induced by carbachol in the subcoeruleus were in the 5- to 8-Hz frequency range. Similar recordings of individual subcoeruleus neurons were carried out in the presence of TTX and the effects of carbachol in the absence of synaptic transmission tested on 41 cells.

In some subcoeruleus cells, the effects of gap junction modulators were tested. Of 9 cells induced to oscillate after carbachol superfusion, the oscillations were blocked in 5 of 5 of these cells by carbenoxolone (300 μM) and in 4 of 4 by mefloquine (10 μM). We also tested the effects of the stimulant modafinil on the input resistance of 9 subcoeruleus cells. Figure 4 shows the changes in input resistance induced by modafinil and their reversal by the gap junction blocker mefloquine on a subcoeruleus neuron.

Of the 124 subcoeruleus cells tested, 60 were depolarized by carbachol, 43 were hyperpolarized, and 7 were not affected. When subcoeruleus cells were divided according to cell type, of the cells depolarized, 25 of 60 had Ia currents, 10 of 60 had LTS currents, and 21 of 60 had Ia+LTS currents. Of the cells hyperpolarized, 23 of 43 had Ia current, 5 of 43 had LTS currents, and 15 of 43 had both. Of the cells not affected, 3 of 7 had Ia currents, 2 of 7 had LTS current, and 2 of 7 had both. Of the cells that were induced to oscillate by carbachol, 3 of 9 had Ia current, 1 of 9 had LTS currents, and 8 of 9 had both.

Cx36 in PPN and Subcoeruleus

Punches from the PPN and subcoeruleus in 400-μm slices were taken at the beginning (10 days) and the end (30 days) of the developmental decrease in REM sleep. Western blot analysis of punches from both PPN and subcoeruleus showed that the levels of Cx36 protein decreased by approximately 75% between 10 and 30 days (Figure 5). The relative levels of Cx36 appeared slightly higher in the PPN than in the subcoeruleus when protein loading was normalized to ß-tubulin, which is known not to change during this period in development.

DISCUSSION

We provide convincing evidence for the presence of electrically coupled pairs of neurons in major nuclei of the RAS, PPN, and subcoeruleus. Moreover, the activity of neurons in these nuclei was induced to fire rhythmically by a cholinergic agonist, presumably mimicking input arising in the PPN, the cholinergic arm of the RAS. In addition, levels of the neuronal gap junction protein Cx36 in these nuclei were detected at high levels early in development and decreased during the developmental decrease in REM sleep. The discovery of electrical coupling in specific RAS cell groups reported here promotes the concept that this underlying process behind specific neurotransmitter interactions modulates ensemble activity across cell populations to promote changes in sleep-wake state. Moreover, the stimulant modafinil was previously found to increase electrical coupling and to decrease input resistance of electrically coupled neurons,[24] suggesting that its excitatory effects may be due to widespread disinhibition of excitatory networks. Modafinil decreased resistance in the presence of fast synaptic blockade in the RAS nuclei tested here.

Electrically Coupled Neurons

Recent imaging studies using voltage-sensitive dyes showed that inhibitory interneurons modulate cortical activation by afferent input.[26] In addition, cortical interneurons exhibit gamma band (~40-Hz) oscillations[10] that are reduced by pharmacologic blockade of gap junctions.[26] The presence of both electrical coupling and chemical synapses between inhibitory interneuron networks is thought to enhance the timing of action potentials.[20-23] In the cortex, electrical coupling may contribute to action potential synchronization and network oscillations, to coordination and reinforcement of inhibitory postsynaptic potentials, and to coincidence detection in inhibitory networks.[27,28] There is extensive electrical coupling in the cortex during development,[29] but epileptiform activity is virtually absent. Therefore, electrical coupling may result in a "shunting effect" by decreasing the input resistance of coupled cells, thereby reducing the excitability of cortical interneurons. Such a shunting effect has been proposed as the mechanism behind the general absence of epileptiform discharges during early postnatal development of the rat neocortex.[30]

Figures 1 and 3 show the presence of electrically coupled pairs of neurons in the PPN and subcoeruleus in the presence of TTX,

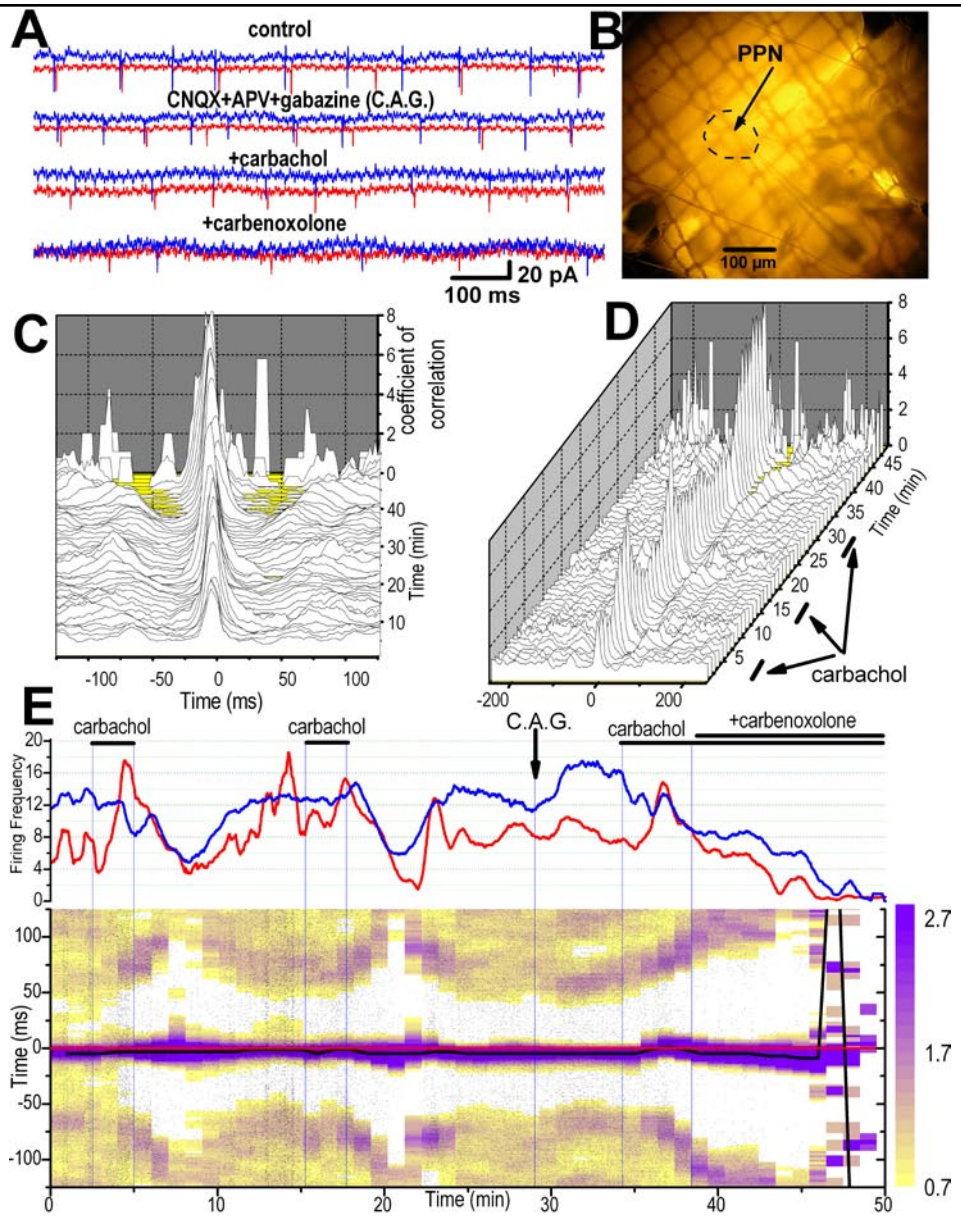

Figure 2—Synchronous activity in 2 pedunculopontine nucleus (PPN) cells, effects of carbachol. Data in this figure were obtained from the same paired recording. **A**. Simultaneous extracellular "loose patch" recordings (1-second samples) were made from 2 cells (red and blue records) in the PPN under different experimental conditions. The occurrence of action potentials in both cells was correlated somewhat in the control, untreated condition (top record), which increased after superfusion with carbachol, and persisted in the presence of fast synaptic blockers (6-cyano-7-nitroquinoxaline-2, 3-dione [CNQX] 10 µM + (±)-2-amino-5-phosphopentanoic acid [APV], 50 µM + gabazine, 10 µM; second record). When carbachol was administered in the presence of these blockers, it induced much higher cross-correlation (third record), but the effect was blocked by adding carbenoxolone (300 µM, bottom record), which desynchronized the cells. **B**. Photograph of the sagittal slice (2× objective) from a 10-day rat showing the location of the PPN where the dual recording was performed. Inferior colliculus is at top right, basis pontis at bottom left. **C**. Sliding 3-D cross-correlogram of action potentials indicated significant synchronous activity throughout 50 minutes of recording. Note that the cross-correlation coefficient peak was near zero time lag and the significant correlation window was around 25 milliseconds (i.e.. the occurrence of action potentials in both cells tended to coincide within a 25-msec interval). Each cross-correlogram was obtained using 2 minutes of data with 1-minute intervals between consecutive cross-correlograms. **D**. Same cross-correlogram as in C but the 3-D graph is tilted in order to view the effect of carbachol on the peaks of coefficient of correlation. The neurons were somewhat correlated at the start, and their correlation increased during carbachol application at 3-7 and 15-18 minutes. The first 2 applications of carbachol were in control aCSF and the third was made in the presence of CNQX+APV+gabazine as in E. Note the sharp increases in correlation with carbachol, especially after fast synaptic blockade. **E**. Upper panel represents a frequency histogram of both cells (red and blue records) throughout the 50 minutes of experiment. Carbachol produced multiphasic responses on the first cell (red) and mainly inhibition on the second cell (blue). Lower panel is a scatter cross-correlation. Each dot represents the interval between an action potential in cell #1 and a given action potential in cell #2 during a time window of ± 125 milliseconds. The color-coded superimposed matrix represents the density of dots and is equivalent to a sliding cross-correlogram. Note that the cross-correlation peak increased in magnitude after each application of carbachol (dark blue indicates higher coefficient of correlation according to the color-coded scale on right). Note also that the peak of correlation (black horizontal line) remained close to center (represented by the horizontal red line) except after application of carbenoxolone, which gradually reduced the activity of the cells and desynchronized them (at 47-50 min). The persistence of a significant cross-correlation coefficient with carbachol in the presence of synaptic blockers and its reduction by carbenoxolone suggest that these cells were coupled by gap junctions.

i.e., in the absence of action potential generation. The frequency of occurrence of coupled cells has been increasing as our methodology improves. Early studies using intracellular recordings estimated that 10% to 15% of RAS cells might be coupled[24]; however, more recent experiments suggest that the locations of coupled neurons might be restricted to the posterior part of the PPN and scattered within subcoeruleus, making the probability higher of obtaining coupled neurons. Using extracellular "loose patch" recordings, we can now identify correlated activity in pairs of cells (as in Figure 2) and then use whole-cell patch clamp to perform recordings on the same cells. These studies now suggest that the proportion of coupled cells in the PPN and subcoeruleus may be in the range of 10% to 30%, although much greater sampling is required to confirm this. Most coupled neurons in the cortex and reticular nucleus appear to be GABAergic.[20-23] Additional recordings followed by processing using various antibodies to immunocytochemically label the recorded neurons are required to determine if noncoupled neurons represent a particular transmitter type or projection pattern, i.e., output cells versus interneurons. Nevertheless, electrical coupling in these RAS nuclei is significant in both occurrence and implication.

Carbachol-Induced Rhythmicity

Our previous study showed that carbachol induced oscillations in some subcoeruleus cells in a wide envelope of frequencies in the theta range.[19] In the presence of fast synaptic blockers, however, carbachol induced synchronization at a very narrow frequency, suggesting that electrical coupling does help synchronize ensemble activity, sharply defining firing rate in these neurons. The present results confirm the ability of carbachol to induce specific oscillations in PPN and subcoeruleus cells (e.g., Figure 3). These oscillations were in the theta range, but it is not clear if that is characteristic of a developing slice at 30°C, or if it would be higher in more developed animals at body temperature. Cholinergic inputs to both PPN and subcoeruleus may provide activation that is shaped by the presence of electrical coupling in the affected neurons.

Modafinil

Modafinil is approved for use in controlling excessive sleepiness in narcolepsy and residual sleepiness in obstructive sleep apnea and as therapy for shift work sleep disorder, but it is also being prescribed "off label" in a number of neuropsychiatric conditions. Virtually all publications on this agent begin by acknowledging that the mechanism of action of modafinil is unknown, but there is general agreement that it increases glutamatergic, adrenergic, and histaminergic, and decreases GABAergic, transmission.[31] However, in a landmark study, modafinil was recently found to increase electrical coupling between cortical interneurons, thalamic reticular neurons, and inferior olivary neurons.[23] Following pharmacologic blockade of connexin permeability, modafinil restored electrotonic coupling. The effects of modafinil were counteracted by the gap junction blocker mefloquine. These authors proposed that modafinil may be acting in a wide variety of cerebral areas by increasing electrotonic coupling in such a way that the high input resistance typical of GABAergic neurons is reduced. These authors proposed that this "shunting effect" of modafinil may activate the whole thalamocortical system by mildly downregulating inhibitory networks while increasing synchronous activation of both interneurons and noninhibitory neurons.[24] Our results show that modafinil may also act on electrically coupled neurons in the RAS, specifically, the PPN and subcoeruleus. This suggests that increasing electrical coupling may promote states of synchronization of sleep-wake rhythms, thus controlling changes in state.

Interestingly, gap junctions can be blocked through membrane fluidization such as that induced by the anesthetic agents halothane and propofol.[32,33] Oleamide promotes sleep and blocks gap junctions. Anandamide enhances adenosine levels to induce sleep and blocks gap junctions.[33] One possibility arising from our finding is that 1 mechanism by which certain agents may induce sleep during "anesthesia" is through blockade of electrical coupling in the RAS. Carbenoxolone, a gap junction blocker, is somnogenic and decreases the synchronicity of gamma oscillations,[34] as well as seizure activity.[35] All of these and similar agents can be expected to block the ability of RAS nuclei to promote ensemble activity, even when individual cells may be firing at fairly high rates. We propose that cholinergic inputs to these neurons induce rhythmic oscillations, but the syncytium of, perhaps GABAergic, electrically coupled cells may be essential to synchronizing sufficient numbers of output cells to project these rhythms to other regions. Much additional work is needed to verify the extent of coupling in the RAS and its role in modulating sleep-wake states. We also need to identify the molecular pathway via which modafinil induces its purported increase in coupling.

Previous studies have shown that both carbenoxolone and mefloquine affect various neuronal processes independently of each other and of their antagonism of gap junction conductance, some of which may be due to effects on astrocytic gap junctions.[36-38] The present study used both carbenoxolone and mefloquine in an attempt to minimize the possible confounding effects of both drugs to modulate the intrinsic properties of the recorded neurons. Additionally, the prior application of fast synaptic blockers or TTX in these experiments would limit these secondary effects.

Cx36 in the RAS

We chose to selectively sample each of the nuclei of interest for Cx36 protein using 400-μm slices, like those used for recordings, and punched 1 mm of PPN and subcoeruleus (without including locus coeruleus) on days 10 and 30, spanning the developmental decrease in REM sleep.[39] Cx36 protein levels at the end of the developmental decrease in REM sleep (day 30) were about 25% of those at day 10. This suggests the presence of a marked developmental decrease in Cx36 protein levels, with considerable amounts of Cx36 protein still present in the adult, suggesting that this gap junction protein may participate in developmental regulation and contribute to sleep-wake control in the adult.

Our previous study on the subcoeruleus used real-time polymerase chain reaction to show that Cx36 mRNA expression and protein levels decreased during the developmental decrease in REM sleep in a few samples.[19] The larger, more specific sample reported herein from subcoeruleus and the new observations on PPN suggest that protein levels in both regions decrease during the developmental decrease in REM sleep (Figure 5). The mechanism that regulates the expression of Cx36 remains to be investigated. Since the level of Cx36 mRNA decreases over age, regulation of Cx36 protein levels is probably at the level of transcriptional control. Changes in intracellular signaling need to be

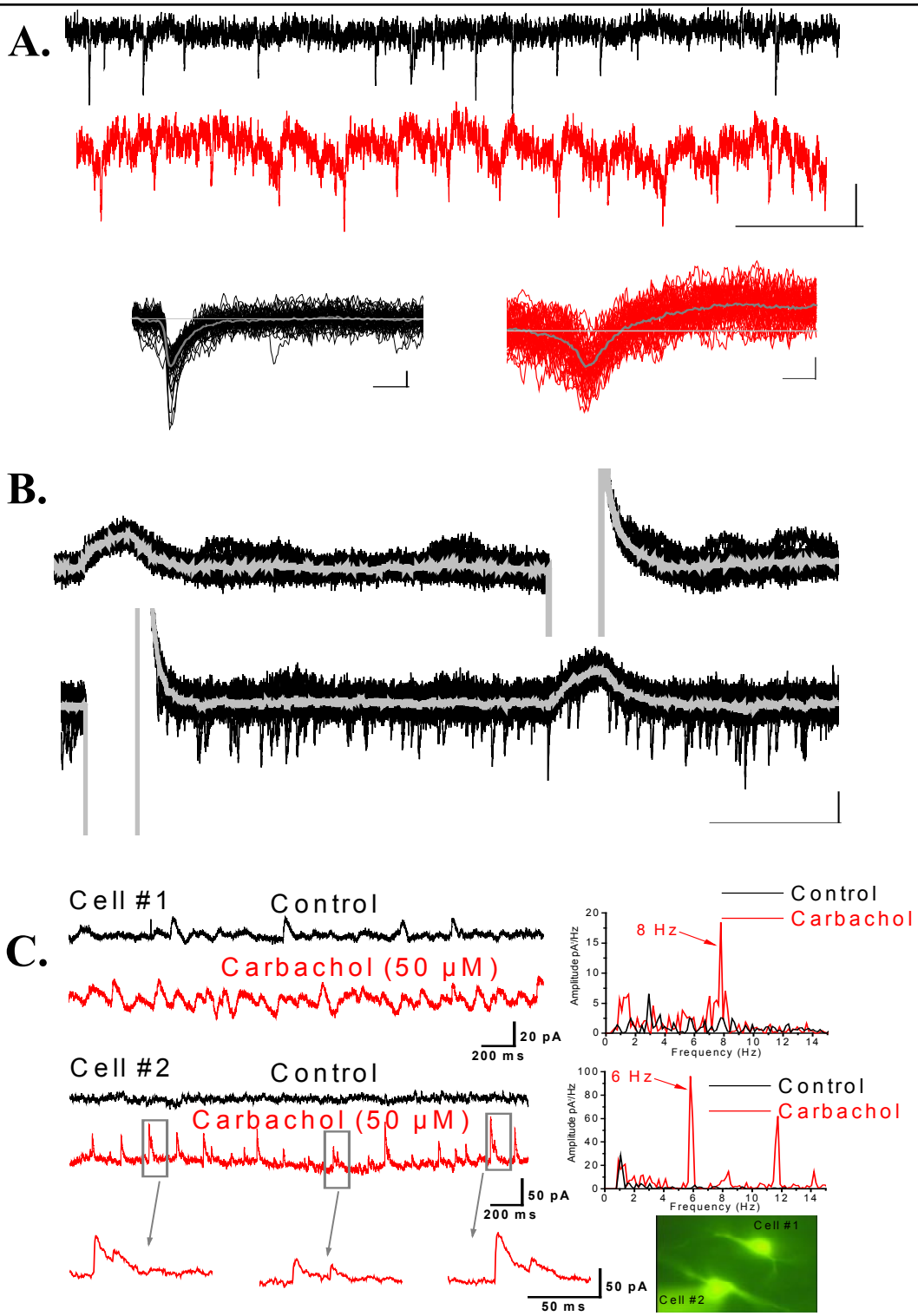

Figure 3—**A**. Spikelets and excitatory postsynaptic currents (EPSC) in the subcoeruleus. Top row, voltage clamp record (holding potential, HP = -50 mV) with spontaneous EPSC. Second row, the same neuron exhibiting spikelets after fast synaptic transmission was blocked (CNQX+APV+gabazine). Third row, overlays (20 sweeps) and averages (gray line) of spontaneous EPSC (left) and spikelets (right) are shown. Note the distinct monophasic shape of the EPSC and the biphasic shape of the spikelets, presumed to represent action potentials filtered by high-resistance gap junctions. **B**. Electrical coupling in the subcoeruleus. During application of tetrodotoxin (TTX, 1 µM), hyperpolarizing current was injected in simultaneously recorded neurons revealing direct electrotonic coupling. A hyperpolarizing step delivered to cell #2, lower record, induced an inward current in cell #1, upper record. Conversely, a hyperpolarizing pulse delivered to cell #1 induced an inward current in cell #2. The coupling coefficient, the response amplitude in the coupled cell divided by the amplitude in the injected cell, for these cells was ~2%. **C**. Carbachol-induced oscillations in subcoeruleus neurons. Simultaneously recorded cells (left side, top records) show little tendency to fire at particular frequencies as evidenced by the power spectrum for each cell (right side). During carbachol superfusion (left side, bottom records), however, both cells showed increased frequency of inhibitory postsynaptic currents (IPSC) as evidenced by the power spectrum for each cell (right side). Note that both cells showed oscillations in the theta frequency but at 8 Hz for cell #1 and 6 Hz for cell #2. On occasion, cell #2 showed doublet IPSC (bottom left), indicating inputs from multiple inhibitory neurons. The inset at bottom right shows the patched neurons fluorescing due to Lucifer yellow infusion from the recording pipettes.

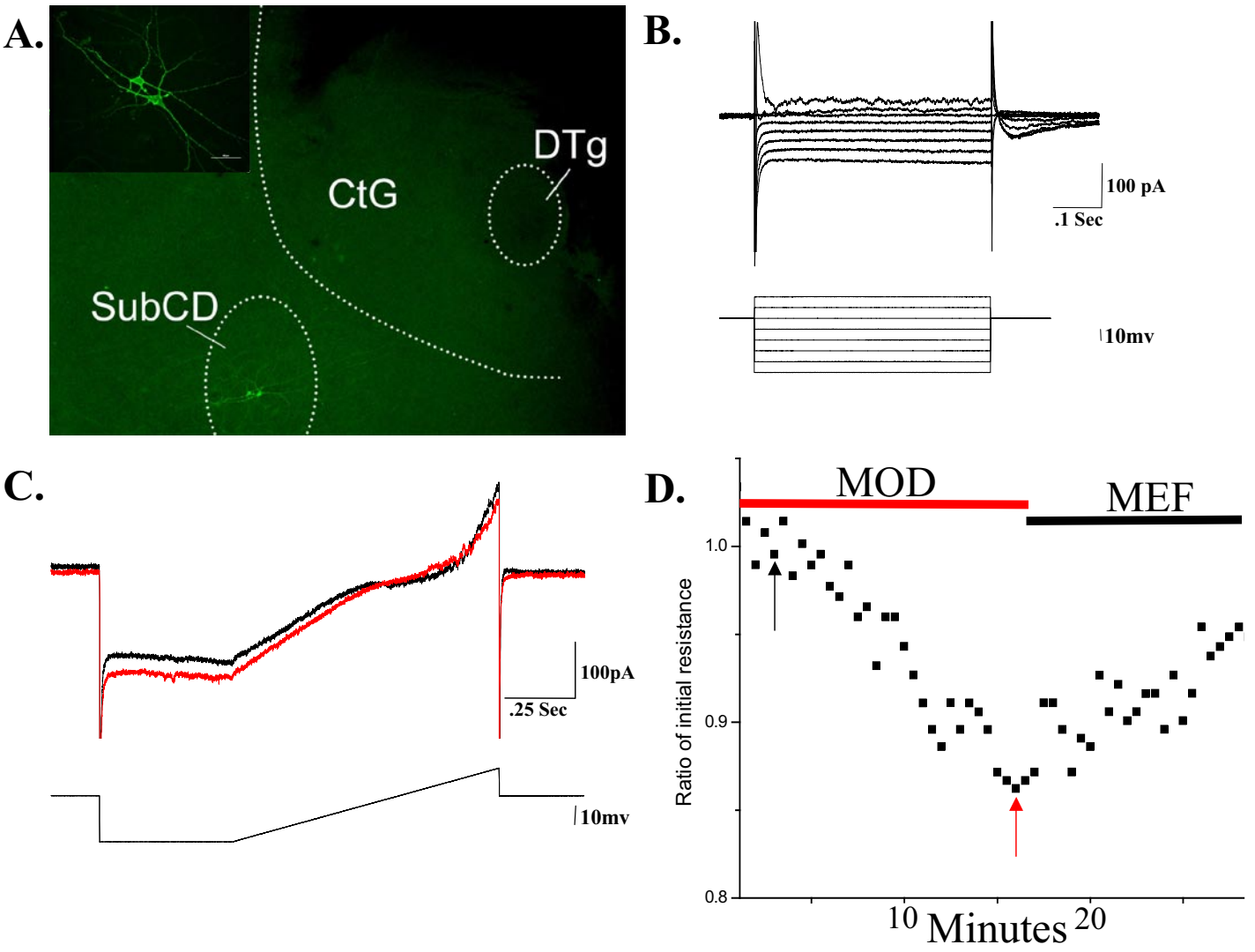

Figure 4—**A**. Location of recorded subcoeruleus neurons. The background is a fluorescence photomicrograph of a slice processed for neurobiotin immunocytochemistry showing the locations of the recorded cells in the subcoeruleus pars D (SubCD, bottom left), the central gray (CtG) and the dorsal tegmental nucleus (DTg) (40X). The inset is a 400X confocal image of the same subcoeruleus cells (calibration bar 50 um). **B**. IV plot of a subcoeruleus cell. Overlayed voltage steps in voltage clamp revealed a putative low threshold spikes (LTS) current and an outward Ia current in this subcoeruleus cell. **C**. Sample recordings revealed a decrease in resistance during modafinil (MOD) application (red record at time marked by red arrow in D), compared to the control condition (black record at time marked by black arrow in D). **D**. Graph of the changes in resistance during modafinil exposure. During application of modafinil, input resistance in the cell shown in B changed from 550 MΩ (black arrow) to 440 MΩ (red arrow), followed by a partial increase during application of mefloquine (MEF). These values are expressed as a ratio of initial resistance.

investigated and how these impact the Cx36 promoter. Other studies need to target manipulation of Cx36 expression and levels to determine changes in REM sleep drive, thus determining if the developmental decrease in REM sleep is driven in whole or in part by a decrement in Cx36.

The questions raised by the discovery of a novel potential mechanism for sleep-wake control are numerous, since this area has received little attention. However, such a mechanism helps explain a multitude of observations and provides a new avenue of research with significant basic and clinical consequences. In summary, our electrophysiological and molecular findings suggest that a significant proportion of subcoeruleus and posterior PPN cells are electrically coupled. We speculate that the overall role of such coupling may be to enhance ensemble rhythmic activity across populations of cells within each nucleus. Although some individual neurons may manifest intrinsic rhythmic firing properties, especially under the influence of cholinergic input, it is the coherence of activity across the population that would be expected to lead to the propagation of rhythms such as are involved in changes in arousal state, e.g., in the transition to waking or REM sleep. Such coherence may be provided by electrical coupling, which acts in concert with well-known neurotransmitter interactions such as reciprocal cholinergic and catecholaminergic modulation. Future studies need to examine how such coupling is organized at the cellular level, how it is enhanced or reduced, and which cell types are involved in these processes.

From a clinical standpoint, dysregulation of electrical coupling can be expected to have wide-ranging effects. If electrical coupling is downregulated in the RAS, then we can expect a decrement in higher-frequency synchronization such as gamma band (40 Hz).

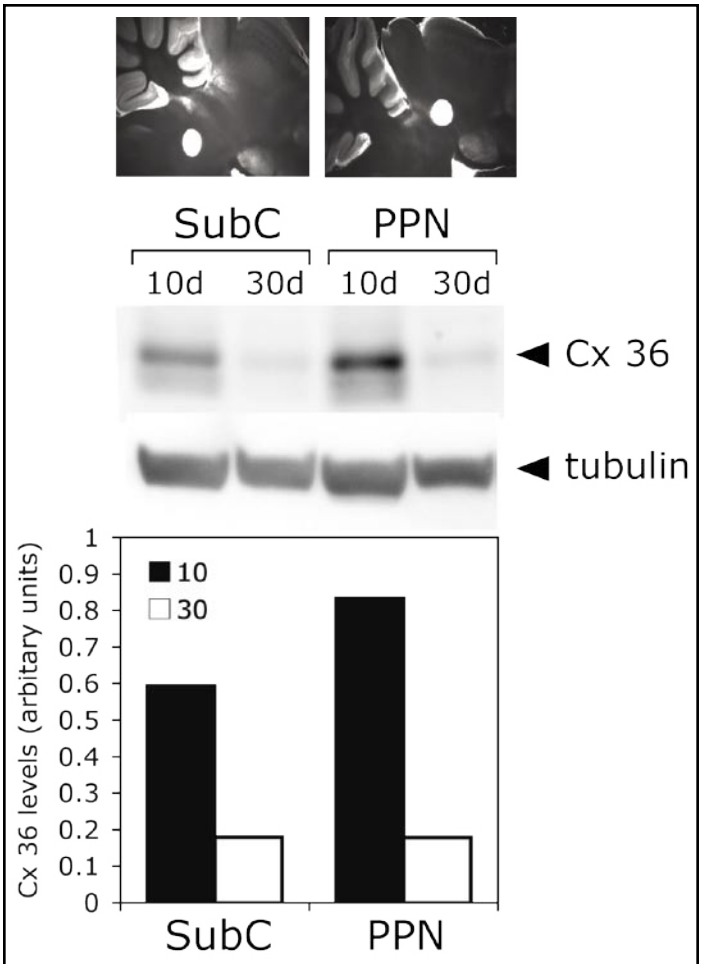

Figure 5—Connexin 36 (Cx36) protein levels in punches of pedunculopontine nucleus (PPN) and subcoeruleus (SubC) at 10 and 30 days (4 rats, 8 bilateral punches of each nucleus pooled/age). Top row shows images of 400-µm sagittal slices punched (1 mm) in the SubC (left, note hole ventral to the locus coeruleus around the seventh nerve), and the posterior PPN (right, note hole ventral to the colliculi). The gels shown are (top row) Cx36 protein from each region in 10-day and 30-day slices and (bottom row) ß-tubulin control for protein loading. The bottom graph shows Cx36 protein levels normalized to ß-tubulin at 10-days and 30-days for SubC (left 2 bars), and PPN (right 2 bars). Note that the amount of protein (a) decreased by about 75% between 10 and 30 days, and (b) both regions showed a decrease, but (c) the absolute amount of Cx36 was higher in PPN and lower in SubC, paralleling the percentage of cells found to manifest spikelets in each nucleus, as described above.

Such a deficit is present in Cx36 knock-out animals.[40] If electrical coupling is upregulated, we can expect increased synchronization of fast rhythms that could lead to increased vigilance and REM sleep drive, such as is evident in disorders like schizophrenia, anxiety disorders, depression, etc.[41] In a disease like REM sleep behavior disorder, which has close links to narcolepsy,[42] the generation of REM sleep does not seem to be impaired, but the atonia during REM sleep seems to be decreased or absent. It is unclear if REM sleep behavior disorder can be modulated by agents that affect gap junctions; however, other parasomnias like restless legs syndrome may be amenable to treatment with such agents, for example, if increased coupling in the inferior olive [see [24]] serves to increase rhythmicity closer to the 10-Hz physiologic tremor and thus smooth out sleep motor dyscontrol.

ACKNOWLEDGMENTS

This work was supported by USPHS grant R01 NS20246 (EGR), F30 NS053163 (DH) and by core facilities of the Center for Translational Neuroscience supported by grant P20 RR20146. We would like to thank Dr. Robert J. Schultz, Drug Synthesis and Chemistry Branch, National Cancer Institute, for the supply of mefloquine.

REFERENCES

1. Wainer BH, Mesulam MM. Ascending cholinergic pathways in the rat brain. In: Brain Cholinergic Systems, Steriade M, Biesold D, eds. New York: Oxford University Press; 1990:65-119.
2. Moruzzi G, Magoun HW. Brain stem reticular formation and activation of the EEG. Electroencephalogr Clin Neurophysiol 1949;1:455-473.
3. Steriade M, Datta S, Pare D, Oakson G, Curro Dossi R. Neuronal activities in brain-stem cholinergic nuclei related to tonic activation processes in thalamocortical systems. J Neurosci 1990;10:2541-2559.
4. Webster H, Jones BE. Neurotoxic lesions of the dorsolateral pontomesencephalic tegmentum-cholinergic cell area in the cat.II. Effects upon sleep-waking states. Brain Res 1988;458:285-302.
5. Shouse M, Siegel JM. Pontine regulation of REM sleep components in cats: integrity of the pedunculopontine tegmentum (PPT) is important for phasic events but unnecessary for atonia during REM sleep. Brain Res 1992;571:50-63.
6. Velazquez-Moctezuma J, Gillin J, Shiromani P. Effect of specific M1, M2 muscarinic receptor agonists on REM sleep generation. Brain Res 1989;503:128-131.
7. Steriade M, McCarley RW. Brainstem Control of Wakefulness and Sleep. 2nd ed. New York: Springer; 2005:728.
8. Reese NB, Garcia-Rill E, Skinner RD. The pedunculopontine nucleus-auditory input, arousal and pathophysiology. Prog. Neurobiol 1995;47:105-133.
9. Smith Y, Sidibe M, Pare J. Synaptic inputs from the substantia nigra and the pedunculopontine nucleus to thalamostriatal neurons in monkeys. Neurosci Abst 2000;26:965.
10. Llinas R, Ribary U. Consciousness and the Brain. The thalamocortical dialogue in health and disease. Ann NY Acad Sci 2001;929:166-175.
11. Mitani A, Ito K, Hallanger AE, Wainer BH, Kataoka K, McCarley RW. Cholinergic projections from the laterodorsal and pedunculopontine tegmental field to the pontine gigantocellular tegmental field in the cat. Brain Res 1988;451:397-402.
12. Shiromani P, Armstrong DM, Gillin JC. Cholinergic neurons from the dorsolateral pons project to the medial pons : a WGA-HRP and choline acetyltransferase immunohistochemical study. Neurosci Lett 1988;95:12-23.
13. Mitler MM, Dement WC. Cataplectic-like behavior in cats after micro-injections of carbachol in pontine reticular formation. Brain Res 1974;68:335-343.
14. Baghdoyan HB, Rodrigo-Angulo RW, McCarley RW, Hobson JA. Site-specific enhancement and suppresion of desynchronized sleep signs following cholinergic stimulation of three brainstem regions. Brain Res 1984:306:39-52.
15. Morrison AR. Paradoxical sleep without atonia. Arch ital Biol 1988;126:275-289.
16. Sanford LD, Morrison AR, Graziella LM, Harris JS, Yoo L, Ross RJ. Sleep patterning and behavior in cats with pontine lesions creating REM without atonia. J Sleep Res 1994;3:233-240.
17. Lu J, Sherman D, Devor M, Saper CB. A putative flip-flop switch for control of REM sleep. Nature 2006;441:589-94.
18. Brown RE, Winston S, Basheer R, Thakkar MM, McCarley RW.

Electrophysiological characterization of neurons in the dorsolateral pontine rapid-eye-movement sleep induction zone of the rat:intrinsic membrane properties and responses to carbachol and orexins. Neuroscience 2006;143:739-755.
19. Heister DS, Hayar A, Charlesworth A, Yates C, Zhou,Y. Garcia-Rill E. Evidence for electrical coupling in the subcoeruleus (SubC) nucleus. J Neurophysiol 2007;97:3142-3147.
20. Connors BW, Long MA. Electrical synapses in the mammalian brain. Annu Rev Neurosci 2000;27:393-418.
21. Hughes SW, Blethyn KL, Cope DW, Crunelli V. Properties and origin of spikelets in thalamocortical neurons in vitro. Neuroscience 2002;3:395-401.
22. Beierlein M, Gibson JR, Connors BW. A network of electrically coupled interneurons drives synchronized inhibition in neocortex. Nat Neurosci 2000;3:904-910.
23. Galarreta M, Hestrin S. Electrical synapses between GABA-releasing interneurons. Nat Reviews Neurosci 2001;2:425-433.
24. Urbano, FJ, Leznik E, Llinas R. Modafinil enhances thalamocortical activity by increasing neuronal electrotonic coupling. Proc Natl Acad Sci 2007;104:12554-12559.
25. Garcia-Rill E, Good CH, Bay KD, Skinner RD. Gap junctions in the developing pedunculopontine nucleus (PPN). Neurosci Abst 2005;31:62.9.
26. Contreras D. and Llinás R. Voltage-sensitive dye imaging of neocortical spatiotemporal dynamics to afferent activation frequency. J Neurosci 2001;21:9403-9413.
27. Traub RD, Kopell N, Bibbig A, Buhl EH, LeBeau FEN, Whittington MA. Gap junctions between interneuron dendrites can enhance synchrony of gamma oscillations in distributed networks. J Neurosci 2001;21:9476-9486.
28. Fricker D. and Miles R. Interneurons, spike timing, and perception. Neuron 2001;32:771-774.
29. Peinado A., Yuste R. and Katz L.C. Extensive dye coupling between rat neocortical neurons during the period of cortical formation. Neuron 1993;10:103-114.
30. Sutor B., Hablitz J.J., Rucker F. and ten Bruggencate G. Spread of epileptiform activity in the immature rat neocortex studied with voltage-sensitive dyes and laser scanning microscopy. J. Neurophysiol 1994;72:1756-1768.
31. Ballon J.S. Feifel D. A systematic review of modafinil: potential clinical uses and mechanisms of action. J Clin Psychiatry 2006;67:554-566.
32. He DS, Burt JM. Mechanism and selectivity of the effects of halothane on gap junction channel function. Circ Res 2000;86:1-10.
33. Evans WH, Boitano S. Connexin mimetic peptides: specific inhibitors of gap-junctional intercellular communication. Bioch Soc Trans 2001;29:606-612.
34. Gigout S, Louvel J, Kawasaki H, et al. Effects of gap junction blockers on human neocortical synchronization. Neurobiol Dis 2006;22:496-508.
35. Gareri P, Condorelli D, Belluardo N, et al. Anticonvulsant effects of carbenoxolone in genetically epilepsy prone rats (GEPRs). Neuropharmacology 2004;47:1205-1216.
36. Cruikshank S, Hopperstad M, Younger M, Connors B, Spray D, Srinivas M. Potent block of Cx36 and Cx50 gap junction channels by mefloquine. Proc Natl Acad Sci 2004;101:12364-12369.
37. Rouach N, Segal M, Koulakoff A, Giaume C, Avignone E. Carbenoxolone blockade of neuronal network activity in culture is not mediated by an action on gap junctions. J Physiol 2003;553:729-745.
38. Thompson AJ, Lochner M, Lummis S. The antimalarial drug quinine, chloroquinine and Mefloquine are antagonists at 5-HT_3 receptors. Br J Pharmacol 2007;151: 666-677.
39. Jouvet-Mounier D, Astic L, Lacote D. Ontogenesis of the states of sleep in rat, cat, and guinea pig during the first postnatal month. Dev Psychobiol 1970;2:216-239.
40. Hormudzi SG, Pais I, LeBeau FEN, Towers SK, Rozov A, Buhl EH, Whittington MA, Monyer H.. Impaired electrical signaling disrupts gamma frequency oscillations in connexin-deficient mice. Neuron 2001;31:487-495.
41. Garcia-Rill E. Disorders of the reticular activating system. Med Hypoth 1997;49:379-387.
42. Schenck CH, Mahowald MW. Rapid eye movement sleep parasomnias. Neurol Clin 2005;23:1107-1126.